Results in Chemistry 30 (2026) 103794

Contents lists available at ScienceDirect

Results in Chemistry

journal homepage: www.sciencedirect.com/journal/results-in-chemistry

Green mechanochemical synthesis of thiazolyl–hydrazone phenolic derivatives and evaluation of their antioxidant activity

Roberto Scipione, Sebastiano Masuri, Ester Sedda, Tiziana Pivetta, Andrea Porcheddu *, Maria Grazia Cabiddu, Andrea Citarella *

Department of Chemical and Geological Sciences, University of Cagliari, Cittadella Universitaria di Monserrato, SS 554, bivio per Sestu, 09042 Monserrato (CA), Italy.

ARTICLE INFO

Keywords:
Phenolic antioxidants
Mechanochemistry
Green synthesis
Telescoped synthesis
Sustainable chemistry
DPPH radical scavenging
ABTS radical scavenging
Heterocycles

ABSTRACT

Oxidative stress plays a pivotal role in the onset and progression of several chronic diseases, prompting the search for novel antioxidant agents. In this context, hydrazone and thiazole scaffolds are particularly attractive due to their ability to stabilize radical intermediates. In the present study, a series of phenolic thiazolyl–hydrazone derivatives was synthesized using a straightforward and sustainable approach. Alongside a conventional solution-phase protocol, a one-pot mechanochemical telescoped strategy was developed for the first time, operating at room temperature with ethanol as a liquid-assisted grinding additive (LAG). The environmental efficiency of both methodologies was evaluated using green metrics, including SPR, PMI, *E*-factor and RME. The mechanochemical approach dramatically reduced solvent consumption (up to 99%), improved the PMI from 35.3 to 2.05, and lowered the *E*-factor from 34.3 to 1.05, while simultaneously increasing overall yields, as observed for ES3 (from 42% to 80%). Antioxidant activity was evaluated using DPPH and ABTS radical-scavenging assays with ascorbic acid as the reference standard. From a biological point of view, electron-rich derivatives exhibited the highest antiradical activity: In particular, the catechol-containing compounds ES26 and ES27 emerged as the most potent derivatives of the series, while ES9, ES16, and ES17 also displayed a favorable antioxidant profile. Notably, the latter compounds outperformed ascorbic acid. Structure–activity relationship analysis highlighted the key role of 3,4-dihydroxy and 3,4-dimethoxy substitution patterns in enhancing radical-scavenging efficiency. Overall, the one-pot mechanochemical sequence represents a rapid, solvent-minimized, energy-efficient and waste-reduced route to phenolic thiazolyl–hydrazone derivatives, enabling access to new compounds with antioxidant activity higher than the reference standard and laying the foundation for future mechanistic and biological investigations.

1. Introduction

Oxidative stress plays a central role in the onset and progression of several pathological conditions, resulting from an imbalance between reactive oxygen/nitrogen species (ROS/RNS) and endogenous antioxidant defenses [1]. The resulting oxidative damage to biomolecules, including lipids, proteins and nucleic acids, has been widely implicated in chronic diseases and aging processes, motivating the search for novel antioxidant agents.

Aromatic hydrazones and thiazole-containing heterocycles are recognized antioxidant scaffolds, given their occurrence in effective radical-scavenging compounds and the ability of sulfur- and nitrogen-containing rings to facilitate hydroperoxide decomposition and metal chelation [2–5]. Hydrazone groups further enhance antioxidant capacity, as the N—H functionality can actively participate in hydrogen atom transfer (HAT) and single-electron transfer (SET) mechanisms, promoting radical scavenging and stabilizing the resulting radical species through electron delocalization and possible coordination effects [6–8]. The introduction of catechol or guaiacol units significantly increases the antioxidant potential, since phenolic moieties favor the stabilization of phenoxy radicals and reduce bond dissociation energies (BDEs) of the O—H bond, thereby facilitating hydrogen donation and improving both HAT- and SET-based antioxidant processes [9–12].

In this context, we present a series of thiazolyl–hydrazones synthesized for the first time exploiting a green mechanochemical approach. These compounds were designed by combining polyphenolic motifs (benzaldehyde, *p*-hydroxybenzaldehyde, vanillin and 3,4-dihydroxybenzaldehyde) with a thiazole core *via* a hydrazone linker. This

* Corresponding authors.
E-mail addresses: andrea.porcheddu@unica.it (A. Porcheddu), andrea.citarella@unica.it (A. Citarella).

https://doi.org/10.1016/j.rechem.2026.103794
Received 7 May 2026; Accepted 25 August 2026
Available online 27 August 2026

methodology drastically reduces solvent consumption and exploits the energy efficiency of the Retsch MM500 laboratory mill, fully aligning with the principles of green chemistry.

2. Results and discussion

2.1. Classical solution-phase synthesis

In the classical solution-phase approach, the target thiazolyl–hydrazone final products were synthesized through a two-step procedure entirely carried out in absolute EtOH (Table 1). In the first step, the corresponding thiosemicarbazones were obtained by a condensation reaction between thiosemicarbazide (5 mmol) and the appropriate benzaldehyde (5 mmol) in EtOH under reflux conditions. The reaction mixture was left stirring at 80 °C for 6 h, leading to the formation of the expected thiosemicarbazone intermediates, which were isolated in good yields (yields 30–71%). The recorded ^{1}H and ^{13}C NMR spectra of the derivatives already reported in the literature are in full agreement with published data, confirming the identity and integrity of the synthesized intermediates. In the second step, each thiosemicarbazone was reacted with an equimolar amount of a suitably substituted phenacyl bromide in EtOH, refluxing the mixture at 80 °C for 6 h. This promoted efficient cyclization and afforded the desired thiazolyl–hydrazone final products (yields 20–96%). A noteworthy exception concerns the derivative bearing a *para*-fluoro substituent on the acetophenone ring: in this case, α-chloroacetophenone was employed instead of the corresponding α-bromo analogue, because of its availability in our laboratory.

Across the series, the isolated yields of the final compounds ranged from 30% to 96%, reflecting good overall efficiency of the conventional synthetic route. All final products were fully characterized by ^{1}H and ^{13}C NMR spectroscopy. Compounds previously known in the literature exhibited spectral data in agreement with the reported values, while the newly synthesized derivatives displayed well-resolved and diagnostically coherent resonances supporting their proposed structures. In all cases, the chemical purity of the isolated compounds exceeded 95% as determined by NMR analysis, underscoring the robustness and reproducibility of this classical synthetic method.

2.2. Green mechanochemical synthesis

To explore a more sustainable and operationally simple route to thiazolyl–hydrazone derivatives, we investigated the feasibility of performing the reaction sequence under mechanochemical conditions. All reactions were conducted using a Retsch MM500 *mixer mill* operating at 30 Hz, using 10 mL zirconia jars equipped with 10 mm zirconia balls under ambient conditions. The study began with the optimization of the first step (A), corresponding to the condensation between aldehyde **1** and thiosemicarbazide **2** to afford the thiosemicarbazone intermediate **3** under liquid-assisted grinding conditions (Table 2). In the absence of a liquid additive (Entry 1), only limited conversion was observed, highlighting the importance of a small amount of liquid to promote efficient

Table 2
Optimization of the mechanochemical sequence. Reactions were performed in a Retsch MM500 mixer mill (30 Hz) using 10 mL zirconia jars equipped with 10 mm zirconia balls at room temperature. AcOH (10 mol%) was used as a catalytic additive whenever reported. η values correspond to liquid-assisted grinding (LAG) conditions. In the telescoped experiments, the jar was opened after completion of step A, reagent **4** was added and milling was resumed without isolation of intermediate **3** and without the need for supplementary solvent.

Entry	Step	LAG (η)[1]	Time	Yield (%)[2]	Notes
1	A	neat	2 h	10	30 Hz, zirconia jar, AcOH (cat.)
2	A	EtOH (η = 1)	2 h	82	30 Hz, zirconia jar, AcOH (cat.)
3	A	AcOH (η = 1)	2 h	87	30 Hz, zirconia jar
4	A	iPrOH (η = 1)	2 h	84	30 Hz, zirconia jar, AcOH (cat.)
5	A	H_2O (η = 1)	2 h	79	30 Hz, zirconia jar, AcOH (cat.)
6	A	H_2O (η = 1)	1 h	45	30 Hz, zirconia jar, AcOH (cat.)
7	A	iPrOH (η = 1)	1 h	83	30 Hz, zirconia jar, AcOH (cat.)
8	A	EtOH (η = 1)	1 h	85	30 Hz, zirconia jar, AcOH (cat.)
9	B	H_2O (η = 1)	1 h	45	30 Hz, zirconia jar
10	B	iPrOH (η = 1)	1 h	85	30 Hz, zirconia jar
11	B	EtOH (η = 1)	1 h	86	30 Hz, zirconia jar
12	B	EtOH (η = 0.2)	1 h	84	30 Hz, zirconia jar
13	A + B	EtOH (η_1 = 1; η_2 = 0.2)	1 h + 1 h	80	30 Hz, zirconia jar, AcOH (cat.)
14	A + B	EtOH (η_1 = 1; η_2 = 0.2)	2 h + 2 h	83	30 Hz, zirconia jar, AcOH (cat.)

Notes: [1]η = μL of liquid additive per mg of total solid reagents (liquid-assisted grinding, LAG); [2]isolated yield.

Table 1
Synthesis of final products of the **ES** series. Reagents and conditions: a) aldehyde (1 equiv), thiosemicarbazide (1 equiv), AcOH (10 mol%, 0.50 mmol, 29 μL), EtOH (15 mL), 80 °C, 6 h, yields 30–71%; b) appropriate acetophenone derivative (1 equiv), EtOH (10 mL), 80 °C, 6 h, second-step isolated yields 20–96%.

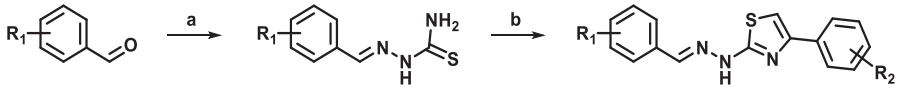

Cmpd	R_1	R_2	Yield (%)
ES3	H	4-Me	90
ES6[1]	H	4-F	66
ES10	H	4-Br	81
ES12	H	4-OMe	58
ES9	H	3,4-diOMe	75
ES22	4-OH	4-Me	90
ES15	3-OMe, 4-OH	4-Me	85
ES23[1]	3-OMe, 4-OH	4-F	30
ES20	3-OMe, 4-OH	4-Br	84
ES17	3-OMe, 4-OH	4-OMe	96
ES16	3-OMe, 4-OH	3,4-diOMe	56
ES28	3,4-diOH	4-Me	90
ES25	3,4-diOH	4-Br	36
ES27	3,4-diOH	4-OMe	33
ES26	3,4-diOH	3,4-diOMe	20

Notes: [1]2-chloro-4′-fluoroacetophenone was used as starting material.

mixing and reactivity. The introduction of an alcohol-based liquid-assisted grinding (LAG) additive significantly improved the reaction outcome, with EtOH (η = 1) providing a substantial increase in yield (Entry 2). Comparable results were obtained using AcOH or iPrOH as LAG additives (Entries 3–4), while water also promoted the reaction, although with slightly lower efficiency (Entry 5). Reducing the milling time led to diminished conversion (Entry 6), although satisfactory yields could still be achieved when using iPrOH or EtOH under optimized conditions (Entries 7–8). With optimized conditions for step A in hand, the second step of the sequence was explored. Step B, involving the cyclization of intermediate **3** with phenacyl bromide **4**, was performed under analogous mechanochemical conditions. Among the tested LAG additives, EtOH again provided the most favorable results (Entry 11), outperforming water (Entry 9) and matching the efficiency observed with iPrOH (Entry 10). Considering its comparable efficiency together with its lower cost and environmental impact, EtOH was selected as the optimal LAG additive for the overall process. Having established suitable conditions for both transformations, we next explored the possibility of performing the sequence in a telescoped mechanochemical protocol. After completion of step A, the milling jar was opened, reagent **4** was added directly and milling was resumed without isolation of intermediate **3**. Under these conditions, the desired product **5** (**ES3**) was obtained in good yield (Entry 13, 80%). Extending the milling time further improved the yield to 83% (Entry 14). Notably, no additional solvent was required for the second step, as the EtOH initially added as LAG remained sufficient to promote the subsequent transformation. The product could be conveniently isolated by simple filtration. Compared with the conventional solution-phase protocol, which typically requires two separate reactions conducted in refluxing EtOH for several hours each, the mechanochemical approach enables the entire sequence to be completed in a significantly shorter time under mild, solvent-minimized conditions. The ability to perform the transformation consecutively in a single milling jar without intermediate isolation highlights the operational simplicity of the method while reducing reaction time and solvent consumption.

Table 3
Ball mill telescoped reactions for the synthesis of the **ES** series. Reagents and conditions: aldehyde (1 equiv), thiosemicarbazide (1 equiv), EtOH (η = 1), AcOH (10 mol%, 0.50 mmol, 29 μL), RT, 1 h; b) appropriate acetophenone derivative (1 equiv), yields 29–93%.

Cmpd	R_1	R_2	Yield (%)
ES3	H	4-Me	80
ES6[1]	H	4-F	29
ES10	H	4-Br	93
ES12	H	4-OMe	91
ES9	H	3,4-diOMe	80
ES22	4-OH	4-Me	84
ES15	3-OMe, 4-OH	4-Me	69
ES23[1]	3-OMe, 4-OH	4-F	64
ES20	3-OMe, 4-OH	4-Br	88
ES17	3-OMe, 4-OH	4-OMe	76
ES16	3-OMe, 4-OH	3,4-diOMe	86
ES28	3,4-diOH	4-Me	92
ES25	3,4-diOH	4-Br	76
ES27	3,4-diOH	4-OMe	85
ES26	3,4-diOH	3,4-diOMe	88

Notes: [1]2-chloro-4′-fluoroacetophenone was used as starting material.

room temperature significantly reduced the energy input, while the telescoped one-jar setup minimized intermediate handling and associated material losses. In addition, the operational simplicity of milling and filtration-based workup contributed to an overall more robust and reproducible process, as further demonstrated by green metrics analysis.

2.3. Reaction scale-up

The robustness of the mechanochemical protocol was further demonstrated through its direct translation to a preparative scale (Scheme 1). The one-pot synthesis of thiazolyl hydrazone **5** was successfully performed on a 20 mmol scale under the same milling frequency and temperature of the smaller scale, without the need for further optimization. Notably, the amount of LAG additive was reduced

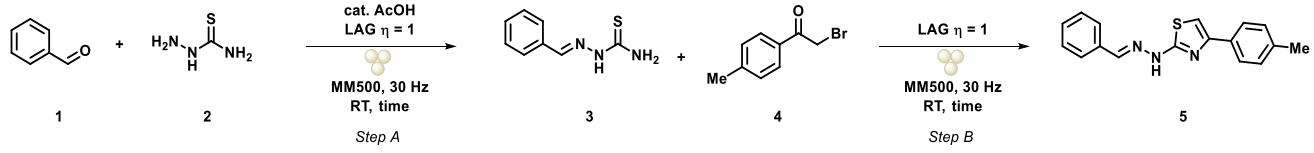

Finally, the optimized telescoped mechanochemical conditions were applied to the synthesis of the same series of substrates, affording the corresponding thiazolyl–hydrazone derivatives in good to excellent yields, thereby demonstrating the generality and robustness of the protocol (Table 3).

to η = 0.25 μL mg^{-1}, while still ensuring efficient mixing and reactivity. The reaction proceeded smoothly in a 50 mL zirconia jar at 30 Hz and room temperature, affording the desired product in 71% isolated yield. Importantly, the multicomponent sequence was carried out in a single milling step without intermediate isolation, confirming the efficiency of

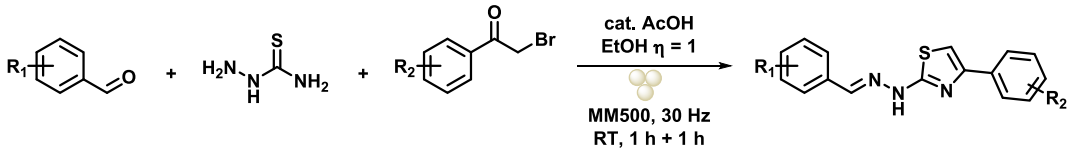

Overall, the mechanochemical protocol led to a marked improvement in the efficiency of the synthetic sequence compared to the classical solution-phase approach. In most cases, comparable or higher isolated yields were obtained under mechanochemical conditions, despite drastically shorter reaction times (1–2 h *vs* 12 h). The elimination of prolonged reflux and the execution of both transformations at the telescoped approach under mechanochemical conditions, even in a larger scale. Product isolation was achieved by simple addition of ethanol followed by filtration, thus avoiding column chromatography purification. The ability to keep efficiency and operational simplicity, using this scale, highlights the practical applicability of the method and its potential for a more sustainable synthesis under solvent-minimized

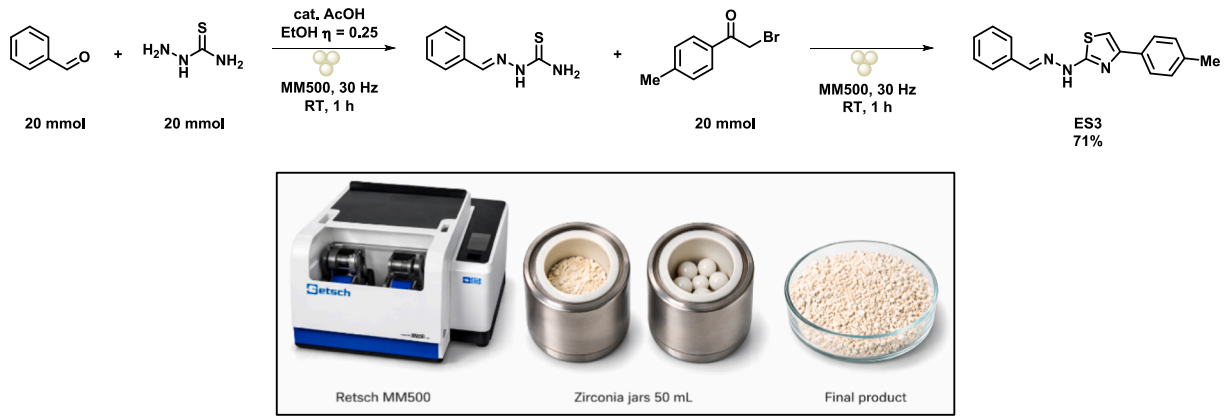

Scheme 1. Mechanochemical telescoped scale-up for the synthesis of **ES3**. The reactions were performed on a 20 mmol scale using a Retsch MM500 mixer mill (30 Hz) in 50 mL zirconia jars equipped with six 10 mm zirconia balls at room temperature. AcOH (10 mol%, 2.0 mmol, 114 μL) was used as a catalytic additive and EtOH as liquid-assisted grinding (LAG) agent (η = 0.25). Representative images of the milling setup (Retsch MM500), zirconia jars, and the isolated product are shown below.

conditions.

2.4. Green metrics calculation

A quantitative comparison of green metrics highlights the substantial sustainability benefits of the mechanochemical protocol (Table 4). For the synthesis of **5** (**ES3**), the classical two-step solution process required 25 mL of EtOH (SPR = 40.8 mL·g^{-1}), whereas the mechanochemical telescoped procedure used only 0.45 mL (SPR = 0.38 mL·g^{-1}), corresponding to a 99% reduction in solvent consumption. The Process Mass Intensity (PMI) decreased dramatically from 35.3 (classical) to 2.05 (mechanochemical), a 17-fold improvement, while the *E*-factor dropped from 34.3 to 1.05, confirming a ~ 33-fold decrease in waste generation. Furthermore, the Reaction Mass Efficiency (RME) increased from 32.3% to 57.1%, reflecting the intrinsic material efficiency of the solvent-minimized, one-jar mechanochemical sequence. Collectively, these metrics demonstrate that the mechanochemical route is not only faster and operationally simpler, but also markedly more sustainable and resource-efficient than the traditional solution-phase synthesis.

2.5. Antioxidant activity

The radical scavenging properties of the synthesized thiazolyl–hydrazone derivatives were evaluated through the 1,1-diphenyl-2-picrylhydrazyl (DPPH) and the 2,2′-azino-bis(3-ethylbenzothiazoline-6-sulfonic acid (ABTS) assays, two validated and widely adopted methods to evaluate the *in vitro* antioxidant activity of natural and synthetic organic molecules. Results are summarized in Table 5. Ascorbic acid was used as reference compound in both assays. In general, both the reference and the tested compounds performed better as ABTS• + radical scavengers than DPPH• ones. This difference may be attributed to the distinct experimental conditions under which the two assays' tests were performed (*e.g.* solvent, reaction time, buffer concentration and pH). Overall, all compounds exhibited a favorable antioxidant profile, with EC_{50} values in the micromolar concentration range. These results suggest that the thiazolyl–hydrazone moiety contributes to the observed antioxidant activity, consistent with the results obtained for similar systems [13–15]. In both assays, compounds bearing the 3,4-dihydroxy motif on R_1 emerged as the most potent radical scavengers of

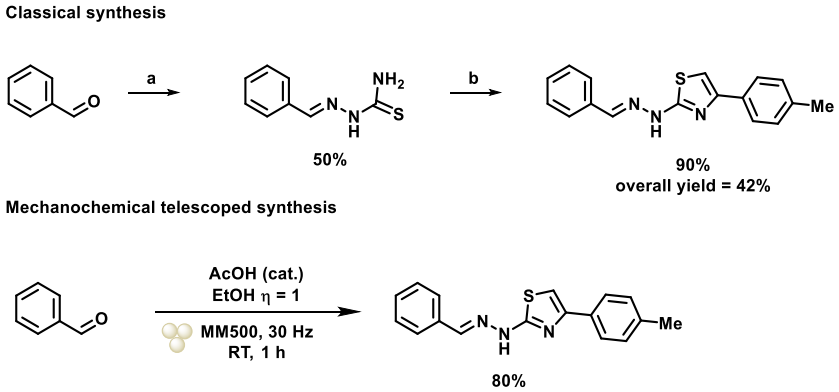

For **ES3**, the mechanochemical telescoped protocol delivered a two-hour, room temperature synthesis using only 0.45 mL EtOH (SPR = 0.38 mL·g^{-1}), compared with 12 h at 80 °C and 25 mL EtOH for the classical route (SPR = 40.8 mL·g^{-1}), corresponding to a 99% reduction in solvent use. The PMI decreased from 35.3 to 2.05 and the *E*-factor from 34.3 to 1.05, while the overall yield increased from 42% (two-step solution) to 80% (one-pot mechanochemistry).

the series. In general, the presence of a catechol-like motif is widely recognized as a key structural feature that enhances the antioxidant activity of compounds across different chemical classes [16–18]. This behavior is particularly emphasized when a electron-releasing group (-OMe) is placed on R_2, as in **ES26** and **ES27**. Notably, compounds **ES9, ES12**, **ES16** and **ES17**, all bearing methoxy groups on R_2 achieved good antioxidant potencies, further supporting the role of these substituents in enhancing the radical-scavenging activity. The presence of electron-

Table 4
Classical two-step *versus* mechanochemical telescoped synthesis of **5** (**ES3**) (green metrics and performance). Classical synthesis reagents and conditions: a) aldehyde (1 equiv), thiosemicarbazide (1 equiv), AcOH (10 mol%), EtOH (15 mL), 80 °C, 6 h; b) appropriate acetophenone derivative (1 equiv), EtOH (10 mL), 80 °C, 6 h. Mechanochemical telescoped synthesis reagents and conditions: a) aldehyde (1 equiv), thiosemicarbazide (1 equiv), EtOH (η = 1), AcOH (10 mol %), RT, 1 h; b) appropriate acetophenone derivative (1 equiv) RT, 1 h.

Parameter	Classical (two-step)	Mechanochemical (telescoped)	Improvement
Input scale (starting material aldehyde)	5 mmol (step 1)	5 mmol (one-pot, 2 steps telescoped)	–
Steps / work-up	2 steps, isolation of the thiosemicarbazone intermediate	2 steps telescoped in one pot, no isolation of the thiosemicarbazone intermediate	Simplified workflow
Time	6 h + 6 h = 12 h	1 h + 1 h = 2 h	−10 h (≈6× faster)
Temperature	80 °C	room temperature	No heating
EtOH used (reaction)	25 mL (15 mL + 10 mL)	0.45 mL (LAG)	−98.2% in volume
Product mass isolated	0.612 g	1.170 g (from 5 mmol, 80%)	–
SPR (mL solvent × g product)	40.8 mL·g^{-1}	0.38 mL·g^{-1}	−99.1%
PMI (Process Mass Intensity)	35.3	2.05	≈ 17× lower
E-factor	34.3	1.05	≈ 33× lower
RME (Reaction Mass Efficiency)	32.3%	57.1%	+77%
Overall isolated yield	42%	80%	+38 p.p.

releasing groups (ERGs) at the 4th position of the thiazole ring has demonstrated to enhance the antioxidant activity of structurally related molecules [14]. Conversely, the introduction of an electron-withdrawing bromine group on R_2 determines a reduction of the antioxidant potency to an extent dependent on the substitution pattern on R_1. Compounds bearing a phenyl or vanillin motif on that position as **ES10** and **ES20** showed higher EC_{50} values than the reference compound. This effect was highly mitigated when the 3,4-dihydroxy moiety was introduced on R_1, as with **ES25**.

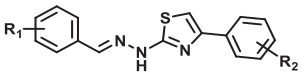

2.6. Computational studies

2.6.1. Structural and electronic properties

The Density Functional Theory (DFT)-optimized geometries of the studied compounds are presented in Fig. 1, using ES26–27 as representative examples. The corresponding optimized geometries of the remaining compounds are available in the Supplementary section (S32–35). Selected structural metrics (bonds, angles, dihedrals) for the DFT-optimized structures of the studied molecules are reported in Tables S1–6. The shapes of the frontier molecular orbitals (SI, S36–38) reveal a high degree of electron delocalization in both the HOMO and LUMO, consistent with the extensive π-conjugation of the system. The analysis of frontier molecular orbital energies indicates that the presence of electron-withdrawing groups (EWGs) at the R_2 position, such as 4-Br, promotes the stabilization of both HOMO and LUMO orbitals, with an

Table 5
EC_{50} values of the final compounds determined from the antioxidant assays. Ascorbic acid was used as reference compound.

Cmpd	R_1	R_2	DPPH EC_{50} ± SEM (μM)[1]	ABTS EC_{50} ± SEM (μM)[1]
ES3	H	4-Me	16.2 ± 0.2	10.2 ± 0.2
ES6	H	4-F	17.8 ± 0.4	9.8 ± 0.2
ES10	H	4-Br	27.2 ± 0.5	20.0 ± 0.2
ES12	H	4-OMe	13.7 ± 0.6	10.9 ± 0.6
ES9	H	3,4-diOMe	10.6 ± 0.4	8.2 ± 0.1
ES22	4-OH	4-Me	9.1 ± 0.2	7.2 ± 0.1
ES15	3-OMe, 4-OH	4-Me	15.4 ± 0.7	13.7 ± 0.1
ES23	3-OMe, 4-OH	4-F	15.7 ± 0.2	11.1 ± 0.2
ES20	3-OMe, 4-OH	4-Br	25.4 ± 0.6	14.5 ± 0.2
ES17	3-OMe, 4-OH	4-OMe	13.1 ± 0.4	11.1 ± 0.3
ES16	3-OMe, 4-OH	3,4-diOMe	10.3 ± 0.2	9.9 ± 0.4
ES28	3,4-diOH	4-Me	9.6 ± 0.2	3.69 ± 0.04
ES25	3,4-diOH	4-Br	12.6 ± 0.1	2.7 ± 0.1
ES27	3,4-diOH	4-OMe	9.0 ± 0.6	2.7 ± 0.1
ES26	3,4-diOH	3,4-diOMe	8.4 ± 0.2	2.59 ± 0.01
Ascorbic acid			18.6 ± 0.6	12.2 ± 0.1

Notes: [1]Each EC_{50} is reported as Mean ± SEM (Standard Error of the Mean, $N_{experiments} = 3$).

effect accompanied by an increase in the HOMO–LUMO energy gap. A similar behavior has been observed in related systems bearing a —Br group [5]. The opposite trend is observed when Electron Releasing Groups (ERGs) are introduced in the same position (*e.g.* 4-OMe, 3,4-diOMe on R_2). An exception is observed for the derivative ES26 (R_2 = 3,4-diOMe), which exhibits slightly lower HOMO and LUMO energies than ES27 (R_2 = 4-OMe). This behavior may be attributed to a partial loss of coplanarity between the -Ph-R_2 moiety and the thiazole ring in ES26, as evidenced by the dihedral angle D(C6–C7–C9–C12), which is 172.90° for ES26 compared to 176.95° for ES27. This reduced coplanarity in ES26 is expected to reduce π-conjugation between the electron-rich Ph-R_2 group and the thiazole core, thereby diminishing electron delocalization and resulting in a slight stabilization of the frontier molecular orbitals. These findings allow to understand the different reactivity observed between the electron-richer (methoxylated) and the electron-poorer (brominated) antioxidant molecules here reported. Molecular orbitals energies and gaps for the studied compounds are reported in Table S7.

2.6.2. Thermochemical descriptors and antioxidant pathways

To gain deeper insight into the preferred pathways through which the studied molecules exert their antioxidant activity, a series of thermochemical descriptors were calculated in both gas phase and solvent media (ethanol, water). These descriptors include Bond Dissociation Enthalpy (BDE), Ionization Potential (IP), Proton Dissociation Enthalpy (PDE), Proton Affinity (PA) and Electron Transfer Enthalpy (ETE). These descriptors are commonly used to describe the three well-known antioxidant pathways: Hydrogen Atom Transfer (HAT), described by BDE; Single Electron Transfer-Proton Transfer (SET-PT), described by IP and PDE; Sequential Proton Loss Electron Transfer (SPLET), described by PA and ETE [19,20]. A more detailed description of such mechanisms, together with the equations used to calculate the related descriptors is provided in the Supplementary section. Results are summarized on Tables S8–S12. Calculated BDE values (Table S8) show how the benzaldehyde derivatives (ES3-6-9-10-12) could exert their antioxidant properties *via* HAT by abstraction of a hydrogen radical (H•) from their

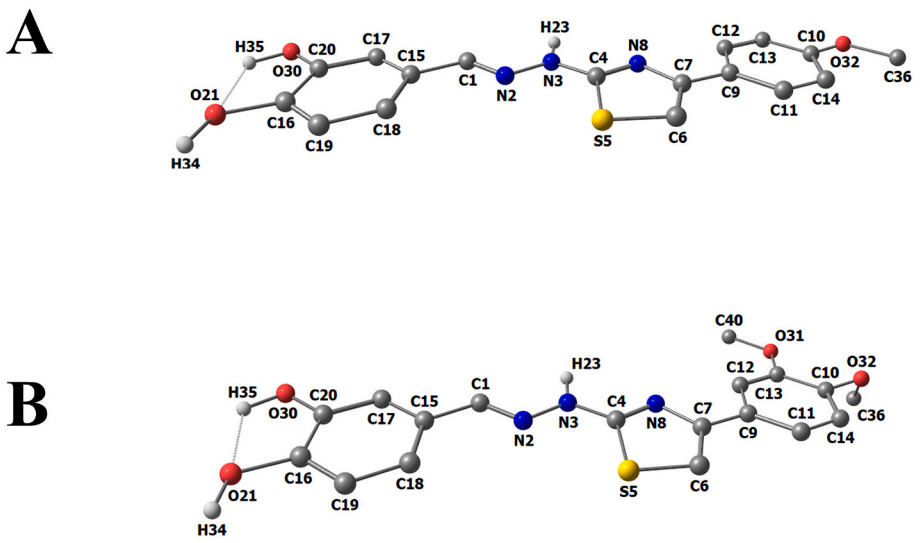

Fig. 1. Molecular structures and atom labelling scheme for ES27 (A) and ES26 (B) at the DFT-optimized geometries (gas phase); C—H bonds are omitted for clarity.

hydrazone NH group. In vanillin-based systems (ES15-16-17-20-23), having R_1 = 3-OMe, 4-OH, the abstraction of H• from the 4-OH position in polar media becomes more competitive than abstraction from the NH group, with average $\Delta(BDE_{4OH}\text{-}BDE_{NH})$ values of about 1.8 and 1.6 Kcal·mol^{-1} in ethanol and water, respectively. This behavior could be attributed to the stabilization of the phenoxy radical through spin density delocalization over the conjugated π-system involving both the hydrazone fragment (—CH═N—NHR—) and the ortho-methoxy group. This effect is evident from the spin density maps, shown for compound ES16 as a representative example (SI, S39). In the derivatives ES25–28, having the 3,4-diOH moiety on R_1, the hydrogen radical abstraction from the 4-OH position becomes thermodynamically more favorable, with average $\Delta(BDE_{4OH}\text{-}BDE_{NH})$ values of about −2.7 and −2.8 Kcal/mol in ethanol and water, respectively. This trend agrees with the BDE values reported for structurally related compounds [14,21]. The observed effect could be attributed to the fact that, in addition to the delocalization effects discussed above for the vanillin derivatives, the phenoxy radical may be further stabilized by the formation of an intramolecular hydrogen bond with the adjacent hydroxyl group (Fig. 2), in analogy with other systems reported in the literature [22–24]. In the same series, H• abstraction from the 3-OH position results less favorable (average $\Delta(BDE_{3OH}\text{-}BDE_{NH})$ of about 5.2 e 4.9 Kcal·mol^{-1} in ethanol and water; average $\Delta(BDE_{3OH}\text{-}BDE_{4OH})$ values of about 7.9 and 7.7 Kcal·mol^{-1} in ethanol and water, respectively). This behavior could be attributed to the reduced delocalization degree of the unpaired electron of the related phenoxy radical, as can be observed from spin density maps, reported for ES26 as example (SI, S40). The calculated IP values (Table S9) are generally higher than the corresponding BDEs, indicating that an electron abstraction from the studied systems is energetically less favorable than the abstraction of an H•. In analogy with results reported for other systems, the presence of a solvent seems to stabilize the radical cation formed upon electron removal, with a consequent decrease of the IP values in solvent media compared with the gas phase [22,25]. As regards the PDE values (Table S10), they are generally higher than the corresponding IP values in the gas phase, whereas the opposite trend is observed in ethanol and water, in agreement with previously reported results [25]. Consequently, in solution the formation of the radical cation represents the energy-determining

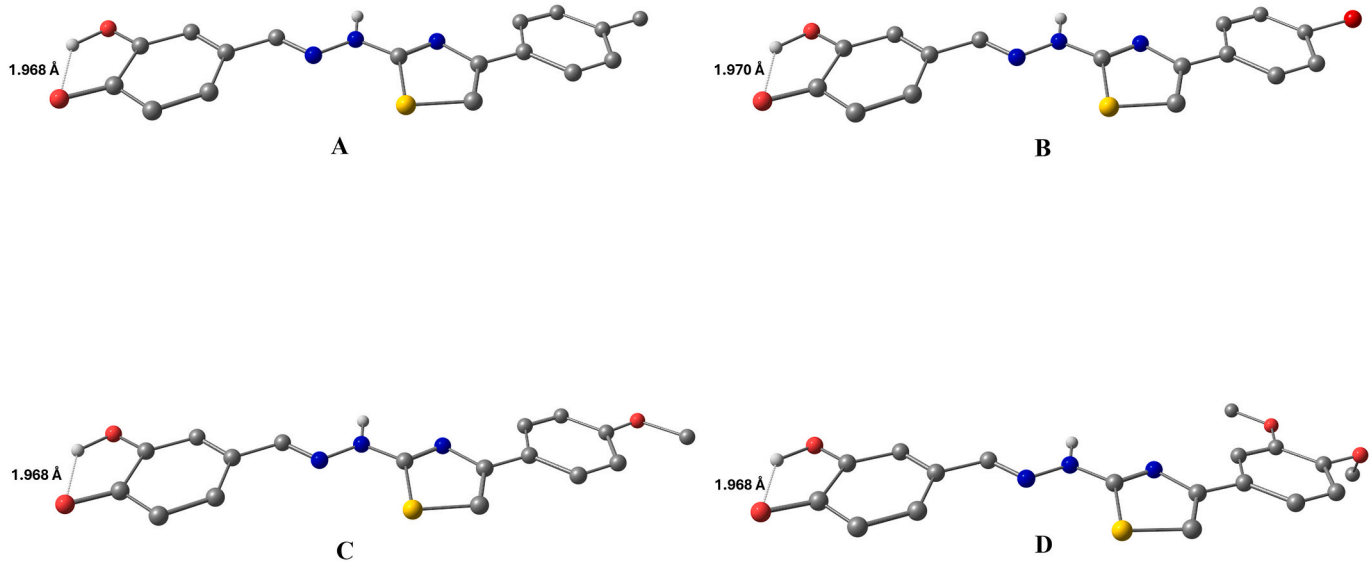

Fig. 2. Molecular structures computed at the DFT level (gas phase) of the ES28 (A), ES25 (B), ES27 (C) and ES26 (D) phenoxy radicals generated by H-atom abstraction from the 4-OH position. C—H bonds were omitted for clarity.

step of the SET-PT, while in the gas phase the subsequent proton dissociation process appears to be the limiting step. Since SET-PT is a two-step process, where the first one (radical cation generation) is energetically less favorable than direct H• abstraction (IPs > BDEs, in both gas phase and solvent media), we can conclude that SET-PT pathway is less preferable from a thermodynamic standpoint than the HAT mechanism, although it becomes more competitive in solvent media. As regards the PA values (Table S11), a marked decrease is observed in solvent media compared with the gas phase. Consistently, the ETE values (Table S12) become higher than the corresponding PA values in ethanol and water, whereas the opposite trend is observed in the gas phase, as seen elsewhere [25]. This behavior could be attributed to the stabilization of the anionic species formed during the first step of the SPLET mechanism by the solvent environment. As a result, proton dissociation is facilitated thermodynamically, while the subsequent electron-transfer process is disfavored due to the enhanced stability of the generated anion. In analogy with BDEs, the deprotonation of the aldehyde in the 4-OH position is more favorable (lower PA values). This trend could be attributed to the formation of an intramolecular hydrogen bond with the vicinal hydroxyl group in the generated anion species (SI, S41). PA values are significantly higher than BDEs in gas phase, while the opposite is observed in solvent media. However, considering that the SPLET pathway is a two-step process, it is important to consider the ETE values as well. Overall, these results suggest that the HAT mechanism is thermodynamically the most favorable pathway in the gas phase. While HAT is expected to remain the dominant antioxidant mechanism in solution, the contribution of the SPLET pathway is likely to become more relevant under solvent conditions. The trends observed for the BDE values also provide a rationale for the experimentally observed increase in antioxidant activity associated with the variation of the structural motif at the R_1 position. These modifications may facilitate hydrogen atom donation by lowering the energy required for homolytic O—H bond cleavage and promoting the stabilization of the resulting radical species.

3. Conclusions

This study establishes for the first time a sustainable and operationally simple route to phenolic thiazolyl–hydrazone derivatives by mechanochemical telescoping of the two key transformations in a single jar (Retsch MM500), completed in 1 h + 1 h at room temperature with 450 μL of EtOH as LAG. In contrast to the classical two-step EtOH reflux (80 °C, 6 h + 6 h), the mechanochemical protocol drastically reduces solvent consumption and energy input while simplifying the workflow. The antioxidant results shows that compounds **ES26** (DPPH: 8.4 ± 0.2 μM, ABTS: 2.59 ± 0.01 μM), **ES27** (DPPH: 9.0 ± 0.6 μM, ABTS: 2.7 ± 0.1 μM) and **ES28** (DPPH: 9.6 ± 0.2 μM, ABTS: 3.69 ± 0.04 μM) are the top performers, with **ES9** (DPPH: 10.6 ± 0.4 μM, ABTS: 8.2 ± 0.1 μM), **ES16** (DPPH: 10.3 ± 0.2 μM, ABTS: 9.9 ± 0.4 μM) and **ES17** (DPPH: 13.1 ± 0.4 μM, ABTS: 11.1 ± 0.3 μM) also surpassing ascorbic acid (DPPH: 18.6 ± 0.6 μM, ABTS: 12.2 ± 0.1 μM). The presence of an electron-rich substituent at R_2 and a catechol or guaiacol moiety at R_1 enhances the antioxidant activity of the studied compounds, as further supported by theoretical investigations. Quantitative green-metrics analysis on **ES3** further substantiates the environmental benefit of mechanochemistry over the conventional route: SPR drops from 40.8 to 0.38 mL·g^{-1}, PMI from 35.3 to 2.05, and *E*-factor from 34.3 to 1.05, while the overall yield increases from ~42% to 80%, demonstrating improved material efficiency and reduced waste at shorter reaction times. Overall, the ability to perform a one-jar, telescoped, solvent-minimized transformation distinguishes this work from previous studies and demonstrates how mechanochemistry can streamline the synthesis of polyphenolic thiazolyl–hydrazones while simultaneously enhancing the environmental profile of the process. Future work will probe mechanistic aspects and explore preliminary biological evaluations to define their translational potential.

CRediT authorship contribution statement

Roberto Scipione: Methodology, Investigation. **Sebastiano Masuri:** Writing – review & editing, Investigation, Data curation. **Ester Sedda:** Validation, Investigation. **Tiziana Pivetta:** Writing – review & editing, Resources, Formal analysis. **Andrea Porcheddu:** Writing – review & editing, Visualization, Supervision, Conceptualization. **Maria Grazia Cabiddu:** Supervision, Resources. **Andrea Citarella:** Writing – review & editing, Writing – original draft, Project administration, Methodology, Formal analysis, Conceptualization.

Declaration of competing interest

The authors declare that they have no known competing financial interests or personal relationships that could have appeared to influence the work reported in this paper.

Acknowledgments

This research did not receive any specific grant from funding agencies in the public, commercial, or not-for-profit sectors. The authors thank the Department of Chemical and Geological Sciences of the University of Cagliari, for access to laboratory facilities and analytical instrumentation. The authors are also grateful to the technical staff of CESAR for their assistance with spectroscopic measurements.

Appendix A. Supplementary data

Supplementary data to this article can be found online at https://doi.org/10.1016/j.rechem.2026.103794.

Data availability

Data will be made available on request.

References

[1] S. Reuter, S.C. Gupta, M.M. Chaturvedi, B.B. Aggarwal, Oxidative stress, inflammation, and cancer: how are they linked? Free Radic. Biol. Med. 49 (2010) 1603–1616, https://doi.org/10.1016/j.freeradbiomed.2010.09.006.

[2] M.A. Gouda, M.A. Berghot, E.A. Baz, W.S. Hamama, Synthesis, antitumor and antioxidant evaluation of some new thiazole and thiophene derivatives incorporated coumarin moiety, Med. Chem. Res. 21 (2012) 1062–1070, https://doi.org/10.1007/s00044-011-9610-8.

[3] F. Lemilemu, M. Bitew, T.B. Demissie, R. Eswaramoorthy, M. Endale, Synthesis, antibacterial and antioxidant activities of thiazole-based Schiff base derivatives: a combined experimental and computational study, BMC Chem. 15 (2021) 67, https://doi.org/10.1186/s13065-021-00791-w.

[4] V.N. Koshelev, O.V. Primerova, S.V. Vorobyev, A.S. Stupnikova, L.V. Ivanova, Synthesis and antioxidant activity of novel thiazole and thiazolidinone derivatives with phenolic fragments, Appl. Sci. 13 (2023) 13112, https://doi.org/10.3390/app132413112.

[5] D. Ungureanu, G. Marc, B. Tiperciuc, C. Moldovan, I. Ionuț, A. Stana, I. Oniga, L. Vlase, A. Pîrnău, O. Oniga, Novel 3,4-dihydroxyphenyl-thiazole-coumarin hybrid compounds: synthesis, in silico and in vitro evaluation of their antioxidant activity, Antioxidants 14 (2025) 636, https://doi.org/10.3390/antiox14060636.

[6] K. Tayade, G.-S. Yeom, S.K. Sahoo, H. Puschmann, S.B. Nimse, A. Kuwar, Exploration of molecular structure, DFT calculations, and antioxidant activity of a hydrazone derivative, Antioxidants 11 (2022) 2138, https://doi.org/10.3390/antiox11112138.

[7] S.A. Aly, S.K. Fathalla, Preparation, characterization of some transition metal complexes of hydrazone derivatives and their antibacterial and antioxidant activities, Arab. J. Chem. 13 (2020) 3735–3750, https://doi.org/10.1016/j.arabjc.2019.12.003.

[8] S.S. Garg, J. Gupta, S. Sharma, D. Sahu, An insight into the therapeutic applications of coumarin compounds and their mechanisms of action, Eur. J. Pharm. Sci. 152 (2020) 105424, https://doi.org/10.1016/j.ejps.2020.105424.

[9] Y.-Z. Zheng, D.-F. Chen, G. Deng, R. Guo, The substituent effect on the radical scavenging activity of apigenin, Molecules 23 (2018) 1989, https://doi.org/10.3390/molecules23081989.

[10] J. Hossen, T.K. Pal, T. Hasan, Theoretical investigations on the antioxidant potential of 2,4,5-trihydroxybutyrophenone in different solvents: a DFT approach, Results Chem. 4 (2022) 100515, https://doi.org/10.1016/j.rechem.2022.100515.

[11] J.P. De La Cruz, M.I. Ruiz-Moreno, A. Guerrero, J.A. López-Villodres, J.J. Reyes, J. L. Espartero, M.T. Labajos, J.A. González-Correa, Role of the catechol group in the

antioxidant and neuroprotective effects of virgin olive oil components in rat brain, J. Nutr. Biochem. 26 (2015) 549–555, https://doi.org/10.1016/j.jnutbio.2014.12.013.
[12] M.R. Antonijević, D.M. Simijonović, E.H. Avdović, A. Ćirić, Z.D. Petrović, J. D. Marković, V. Stepanić, Z.S. Marković, Green one-pot synthesis of coumarin-hydroxybenzohydrazide hybrids and their antioxidant potency, Antioxidants 10 (2021) 1106, https://doi.org/10.3390/antiox10071106.
[13] A.C. Corona, G. Marc, I. Ionuț, C. Moldovan, I. Fizeșan, A.E. Petru, I.V. Creștin, A. Pîrnău, L. Vlase, O. Oniga, Synthesis, cytotoxicity and antioxidant activity evaluation of some thiazolyl–catechol compounds, Antioxidants 13 (2024) 937, https://doi.org/10.3390/antiox13080937.
[14] G. Marc, A. Stana, M. Tertiș, C. Cristea, A. Ciorîță, Ș.-M. Drăgan, V.-A. Toma, R. Borlan, M. Focșan, A. Pîrnău, L. Vlase, S. Oniga, O. Oniga, Discovery of new hydrazone-thiazole polyphenolic antioxidants through computer-aided design and in vitro experimental validation, Int. J. Mol. Sci. 24 (2023) 13277, https://doi.org/10.3390/ijms241713277.
[15] M.S. Shah, M.M. Rahman, M.D. Islam, A. Al-Macktuf, J.U. Ahmed, H. Nishino, M. A. Haque, Synthesis, antimicrobial and antioxidant evaluation with in silico studies of new thiazole Schiff base derivatives, J. Mol. Struct. 1248 (2022) 131465, https://doi.org/10.1016/j.molstruc.2021.131465.
[16] M. Roussaki, K. Zelianaios, E. Kavetsou, S. Hamilakis, D. Hadjipavlou-Litina, C. Kontogiorgis, T. Liargkova, A. Detsi, Structural modifications of coumarin derivatives: determination of antioxidant and lipoxygenase (LOX) inhibitory activity, Bioorg. Med. Chem. 22 (2014) 6586–6594, https://doi.org/10.1016/j.bmc.2014.10.008.
[17] C.A. Rice-Evans, N.J. Miller, G. Paganga, Structure-antioxidant activity relationships of flavonoids and phenolic acids, Free Radic. Biol. Med. 20 (1996) 933–956, https://doi.org/10.1016/0891-5849(95)02227-9.
[18] D.A. Burmistrova, A. Galustyan, N.P. Pomortseva, K.D. Pashaeva, M.V. Arsenyev, O.P. Demidov, M.A. Kiskin, A.I. Poddel'sky, N.T. Berberova, I.V. Smolyaninov, Synthesis, electrochemical properties, and antioxidant activity of sterically hindered catechols with 1,3,4-oxadiazole, 1,2,4-triazole, thiazole or pyridine fragments, Beilstein J. Org. Chem. 20 (2024) 2378–2391, https://doi.org/10.3762/bjoc.20.202.
[19] Z. Marković, J. Tošović, D. Milenković, S. Marković, Revisiting the solvation enthalpies and free energies of the proton and electron in various solvents, Comput. Theor. Chem. 1077 (2016) 11–17, https://doi.org/10.1016/j.comptc.2015.09.007.
[20] J. Rimarčík, V. Lukeš, E. Klein, M. Ilčin, Study of the solvent effect on the enthalpies of homolytic and heterolytic N–H bond cleavage in p-phenylenediamine and tetracyano-p-phenylenediamine, J. Mol. Struct. THEOCHEM 952 (2010) 25–30, https://doi.org/10.1016/j.theochem.2010.04.002.
[21] M. Mic, A. Pîrnău, C.G. Floare, R. Borlan, M. Focsan, O. Oniga, M. Bogdan, L. Vlase, I. Oniga, G. Marc, Antioxidant activity evaluation and assessment of the binding affinity to HSA of a new catechol hydrazinyl-thiazole derivative, Antioxidants 11 (2022) 1245, https://doi.org/10.3390/antiox11071245.
[22] J.B. Veselinović, A.M. Veselinović, Ž.J. Vitnik, V.D. Vitnik, G.M. Nikolić, Antioxidant properties of selected 4-phenyl hydroxycoumarins: integrated in vitro and computational studies, Chem. Biol. Interact. 214 (2014) 49–56, https://doi.org/10.1016/j.cbi.2014.02.010.
[23] S. Masuri, M.G. Cabiddu, E. Cadoni, T. Pivetta, Hydroxylated 3-(pyridin-2-yl) coumarins as radical scavengers with potent lipoxygenase inhibitor activity, New J. Chem. 45 (2021) 10749–10760, https://doi.org/10.1039/D1NJ01232K.
[24] G. Mazzone, N. Malaj, A. Galano, N. Russo, M. Toscano, Antioxidant properties of several coumarin–chalcone hybrids from theoretical insights, RSC Adv. 5 (2015) 565–575, https://doi.org/10.1039/C4RA11733F.
[25] M. Demurtas, V. Onnis, P. Zucca, A. Rescigno, J.I. Lachowicz, L. De Villiers Engelbrecht, M. Nieddu, G. Ennas, A. Scano, F. Mocci, F. Cesare Marincola, Cholinium-based ionic liquids from hydroxycinnamic acids as new promising bioactive agents: a combined experimental and theoretical investigation, ACS Sustain. Chem. Eng. 9 (2021) 2975–2986, https://doi.org/10.1021/acssuschemeng.1c00090.